Supporting Information

Harvesting Energy from Water Evaporation: A Green Power Device Printed from Waste Bamboo

*Chenhong Xu[a], Yuanjie Wei[a], Qun Liu[a], Quancai Li[a], Xin Guo[a], Qian Wang[a], Ziyi Gong[a], Hehe Ren[a], Jian Zou[a], Jing Liang[a, b], Wei Wu[a, b]**

[a] Laboratory of Printable Functional Materials and Printed Electronics, School of Physics and Technology, Wuhan University, Wuhan 430072, P. R. China

[b] Research Center for Printed Electronics and Smart Wearable Systems, School of Future Technology, Wuhan Textile University, Wuhan 430200, P. R. China

Correspondence:

weiwu@whu.edu.cn (W. Wu)

To whom correspondence should be addressed: +86-27-68778491. Fax: +86-27-68778491.
weiwu@whu.edu.cn (W. Wu)

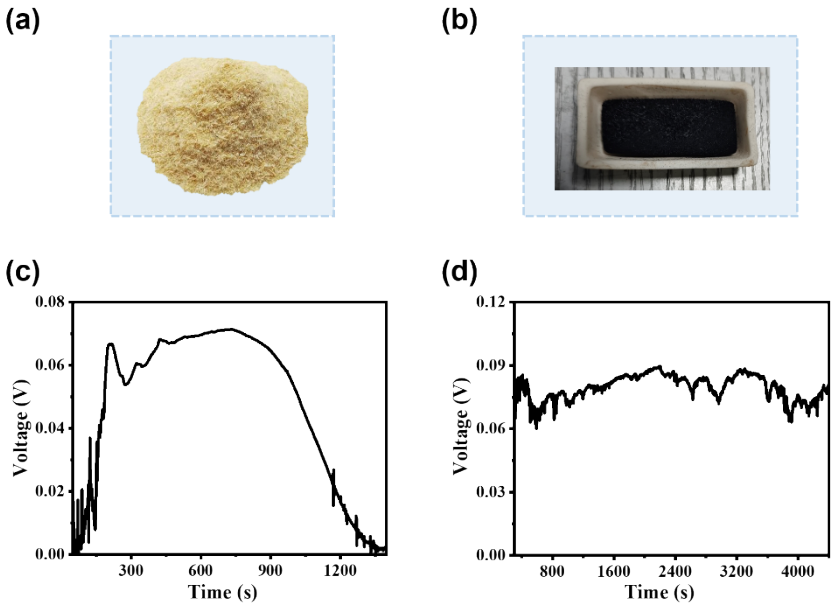

Fig. S1 (a) Photographs showing the natural waste bamboo sawdust and (b) the resulting bamboo-derived carbon after high-temperature treatment. (c) Variation in open-circuit voltage during the drying process under ambient conditions after water is added to a doctor-bladed film prepared from an aqueous dispersion of bamboo-derived carbon. (d) Change in open-circuit voltage when a section of the doctor-bladed film is partially immersed in water.

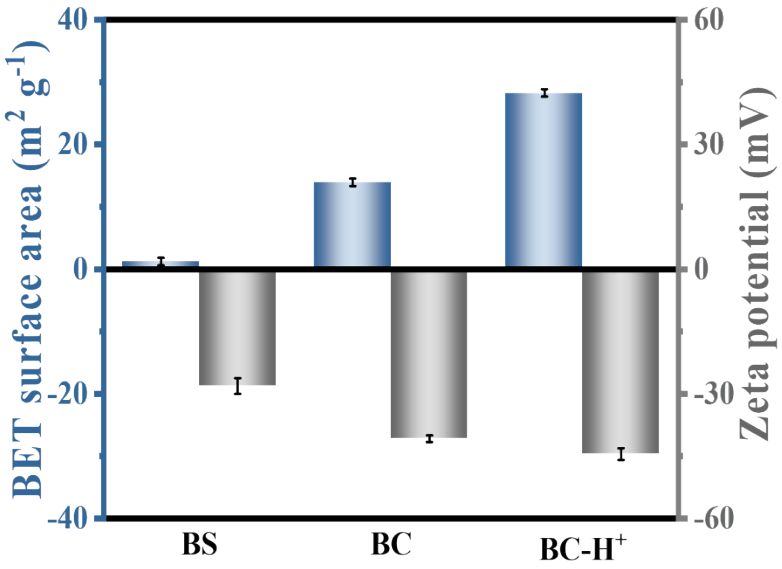

Fig. S2 Comparative analysis of BET surface area and zeta potential for BS, BC, and BC-H^+.

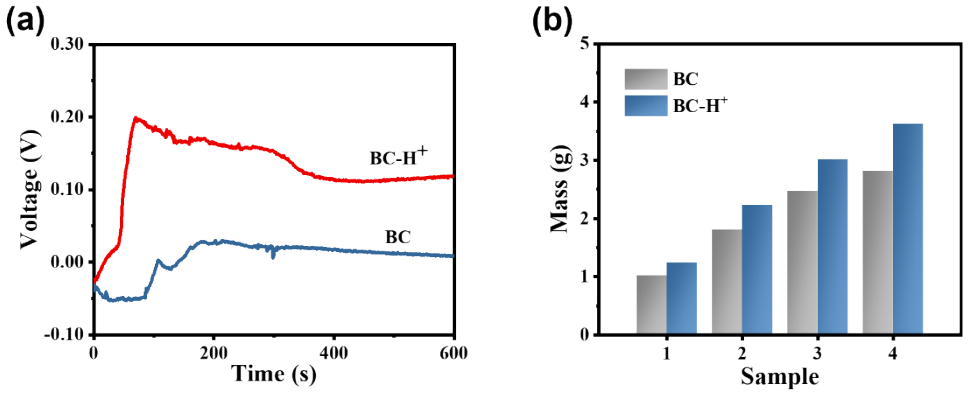

Fig. S3 Effects of acidification treatment on bamboo-derived charcoal. (a) Alterations in evaporation-induced power generation performance before and after acidification. (b) Changes in mass of the charcoal material following the acidification process.

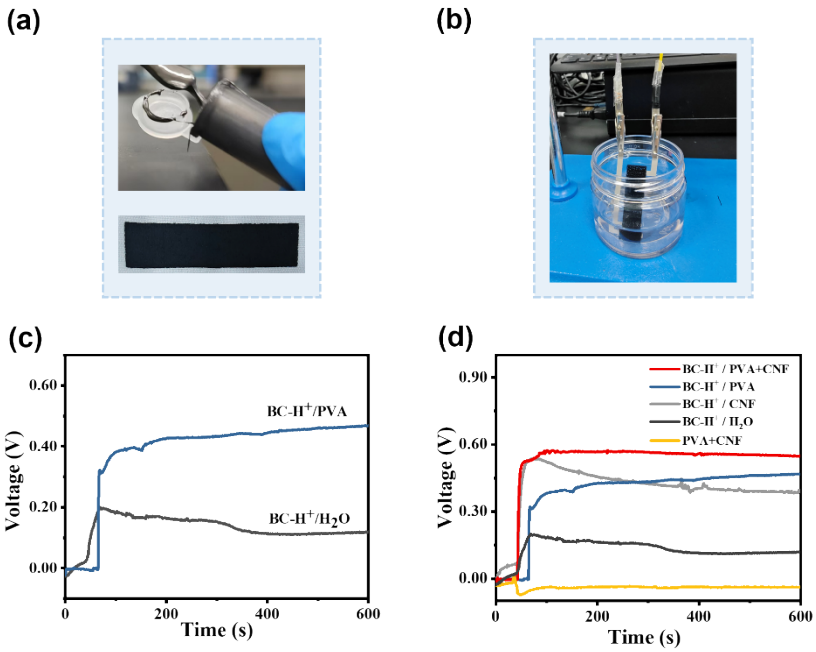

Fig. S4 Performance evolution of BC-H^+ formulated into functional ink. (a) Photograph depicting the BC-H^+ ink prepared for printing applications. (b) Devices fabricated *via* screen-printing using the BC-H^+ ink. (c) Open-circuit voltage comparison between an aqueous BC-H^+ solution and the formulated BC-H^+ ink. (d) Open-circuit voltage of BC-H^+ inks prepared with varying binder compositions.

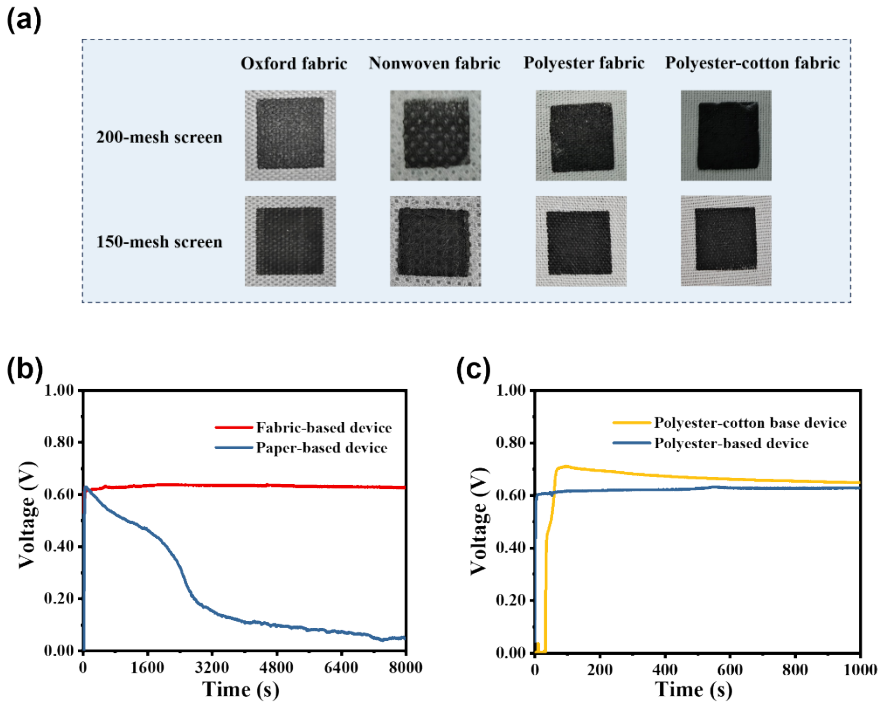

Fig. S5 Impact of different printing substrates on BC-H^+ devices. (a) Photographs showing BC-H^+ ink patterns fabricated using 150-mesh and 200-mesh screens on different textile materials. (b) Open-circuit voltage recorded from BC-H^+ films deposited on fabric-based and paper-based substrates. (c) Open-circuit voltage of BC-H^+ films prepared on nylon and polyester textile substrates.

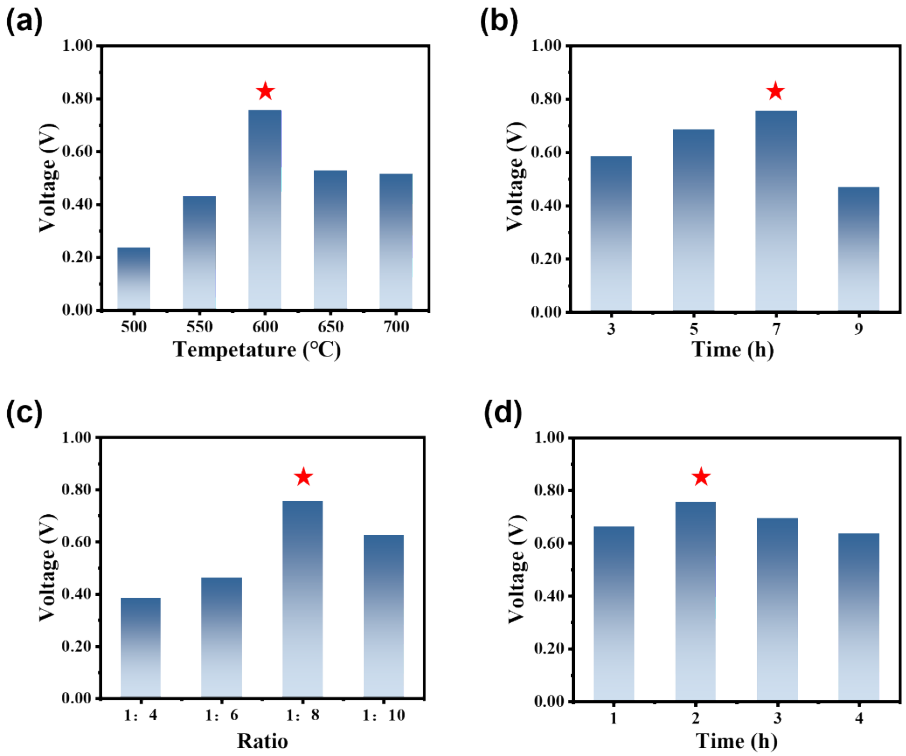

Fig. S6 The power generation performance of BC-H^+ membranes through evaporation is influenced by carbonization and acidification processes. (a) Open-circuit voltage of BC-H^+ membranes fabricated at varying carbonization temperatures. (b) Open-circuit voltage of BC-H^+ membranes prepared with different carbonization durations. (c) Open-circuit voltage of BC-H^+ membranes subjected to varying acidification ratios. (d) Open-circuit voltage of BC-H^+ membranes treated with different acidification times.

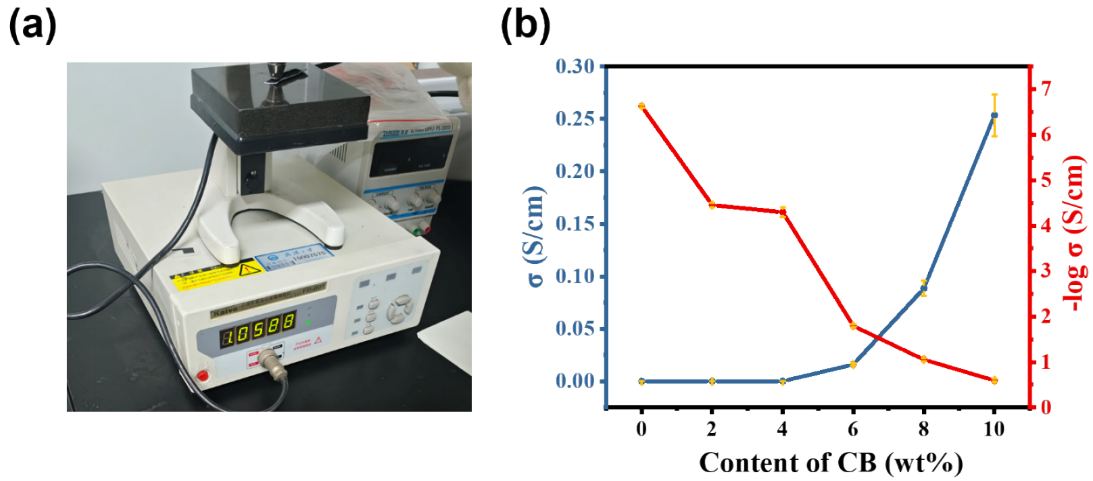

Fig. S7 Electrical conductivity of composite membranes under different CB contents.

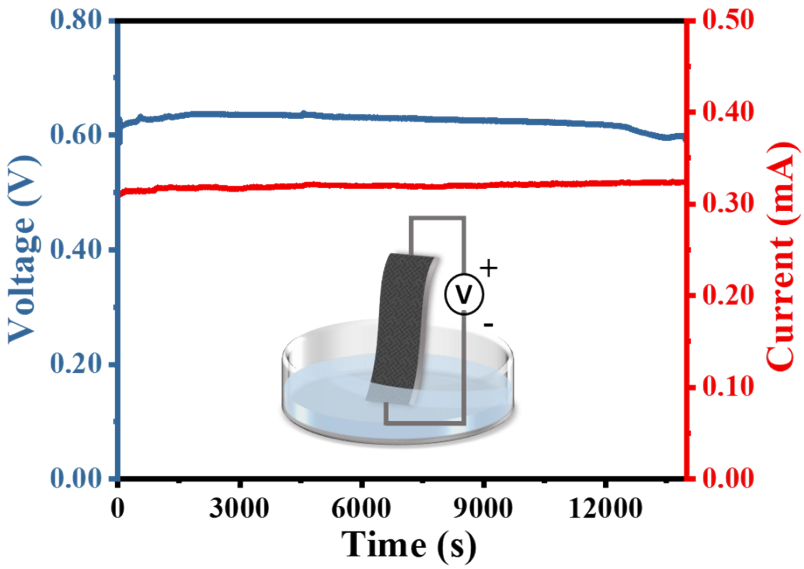

Fig. S8 Open-circuit voltage (left) and short-circuit current (right) of the optimized device in deionized water.

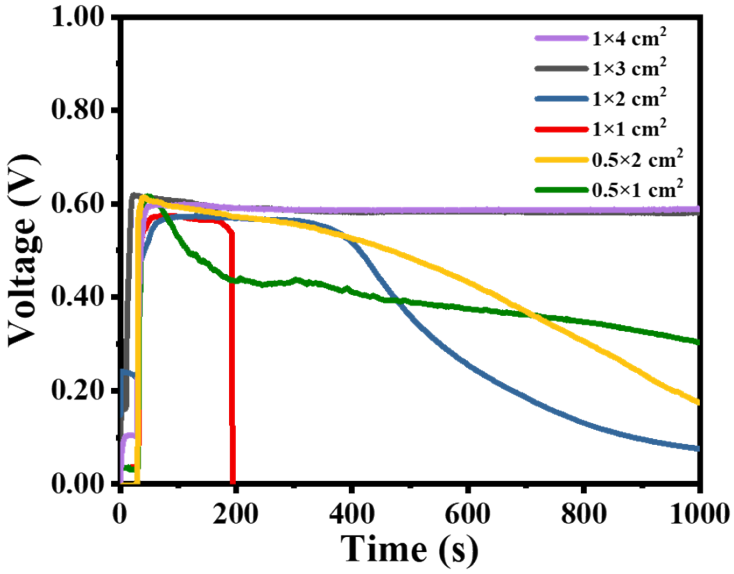

Fig. S9 The temporal evolution of open-circuit voltage for BC-H^+ membranes with varying active areas.

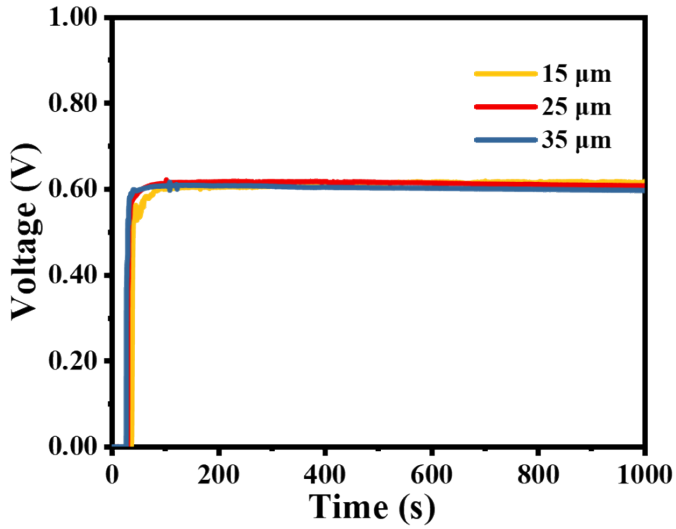

Fig. S10 The open-circuit voltage variations of proton exchange membranes with different thicknesses.

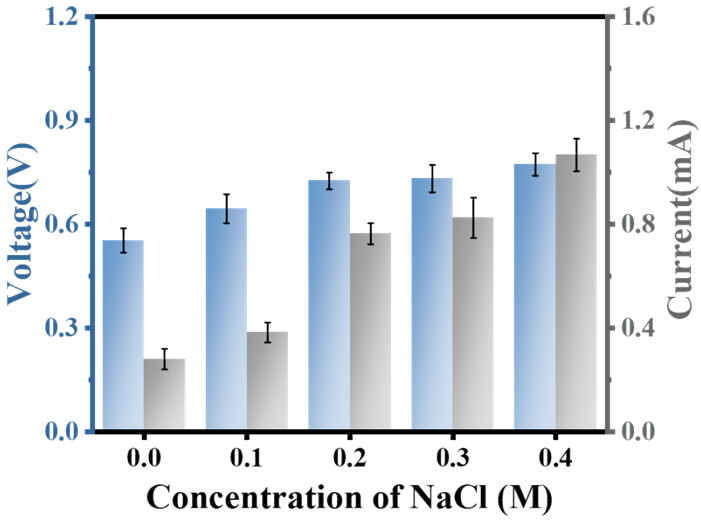

Fig. S11 Variations in voltage and current of the device measured in NaCl solutions with concentrations ranging from 0 to 0.4 M.

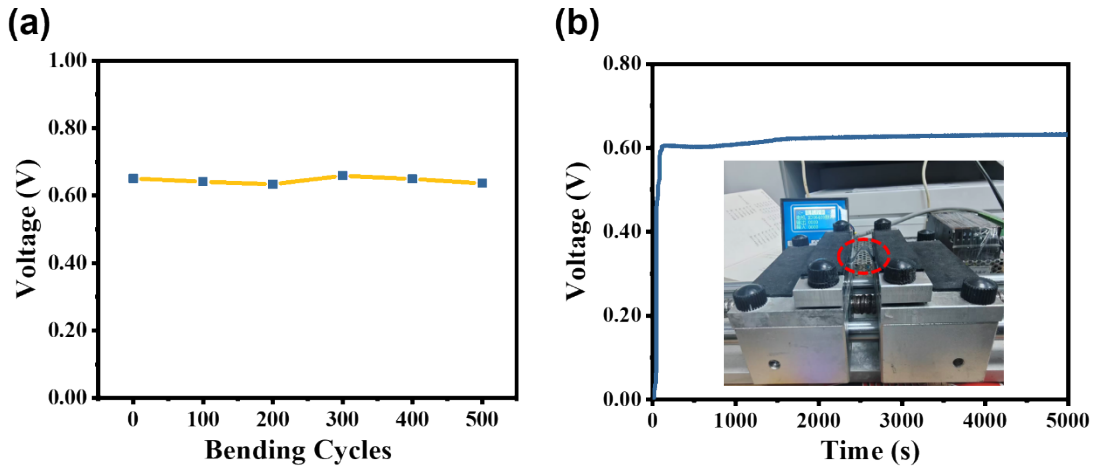

Fig. S12 (a) Output voltage of the device under different bending cycle times. (b) The variation of the output voltage of the device over time after 500 cycles of bending.

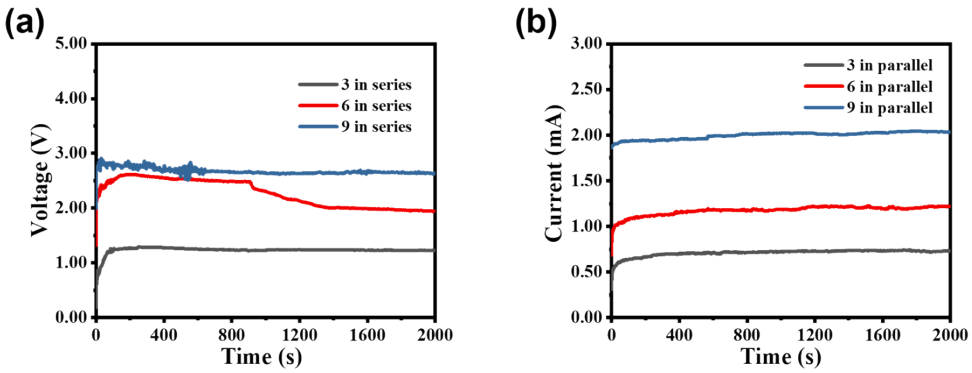

Fig. S13 The effects of series or parallel connections on voltage and current with varying numbers of devices.